Search for charged Higgs bosons in e^+e^- collisions at $\sqrt{s} = 181–184$ GeV

ALEPH Collaboration

R. Barate, D. Decamp, P. Ghez, C. Goy, S. Jezequel, J.-P. Lees, F. Martin, E. Merle, M.-N. Minard, J.-Y. Nief, B. Pietrzyk

Laboratoire de Physique des Particules (LAPP), IN2P3-CNRS, F-74019 Annecy-le-Vieux Cedex, France

R. Alemany, M.P. Casado, M. Chmeissani, J.M. Crespo, M. Delfino, E. Fernandez, M. Fernandez-Bosman, Ll. Garrido [1], E. Graugès, A. Juste, M. Martinez, G. Merino, R. Miquel, Ll.M. Mir, P. Morawitz, A. Pacheco, I.C. Park, A. Pascual, I. Riu, F. Sanchez

Institut de Física d'Altes Energies, Universitat Autònoma de Barcelona, 08193 Bellaterra (Barcelona), Spain [2]

A. Colaleo, D. Creanza, M. de Palma, G. Gelao, G. Iaselli, G. Maggi, M. Maggi, S. Nuzzo, A. Ranieri, G. Raso, F. Ruggieri, G. Selvaggi, L. Silvestris, P. Tempesta, A. Tricomi [3], G. Zito

Dipartimento di Fisica, INFN Sezione di Bari, I-70126 Bari, Italy

X. Huang, J. Lin, Q. Ouyang, T. Wang, Y. Xie, R. Xu, S. Xue, J. Zhang, L. Zhang, W. Zhao

Institute of High-Energy Physics, Academia Sinica, Beijing, China [4]

D. Abbaneo, U. Becker [5], G. Boix [6], M. Cattaneo, V. Ciulli, G. Dissertori, H. Drevermann, R.W. Forty, M. Frank, F. Gianotti, A.W. Halley, J.B. Hansen, J. Harvey, P. Janot, B. Jost, I. Lehraus, O. Leroy, C. Loomis, P. Maley, P. Mato, A. Minten, A. Moutoussi, F. Ranjard, L. Rolandi, D. Rousseau, D. Schlatter, M. Schmitt [7], O. Schneider [8], W. Tejessy, F. Teubert, I.R. Tomalin, E. Tournefier, M. Vreeswijk, A.E. Wright

European Laboratory for Particle Physics (CERN), CH-1211 Geneva 23, Switzerland

Z. Ajaltouni, F. Badaud, G. Chazelle, O. Deschamps, S. Dessagne, A. Falvard,
C. Ferdi, P. Gay, C. Guicheney, P. Henrard, J. Jousset, B. Michel, S. Monteil,
J-C. Montret, D. Pallin, P. Perret, F. Podlyski

Laboratoire de Physique Corpusculaire, Université Blaise Pascal, IN2P3-CNRS, Clermont-Ferrand, F-63177 Aubière, France

J.D. Hansen, J.R. Hansen, P.H. Hansen, B.S. Nilsson, B. Rensch, A. Wäänänen

Niels Bohr Institute, 2100 Copenhagen, Denmark [9]

G. Daskalakis, A. Kyriakis, C. Markou, E. Simopoulou, A. Vayaki

Nuclear Research Center Demokritos (NRCD), GR-15310 Attiki, Greece

A. Blondel, J.-C. Brient, F. Machefert, A. Rougé, M. Swynghedauw, R. Tanaka,
A. Valassi [10], H. Videau

Laboratoire de Physique Nucléaire et des Hautes Energies, Ecole Polytechnique, IN2P3-CNRS, F-91128 Palaiseau Cedex, France

E. Focardi, G. Parrini, K. Zachariadou

Dipartimento di Fisica, Università di Firenze, INFN Sezione di Firenze, I-50125 Firenze, Italy

R. Cavanaugh, M. Corden, C. Georgiopoulos

Supercomputer Computations Research Institute, Florida State University, Tallahassee, FL 32306-4052, USA [11,12]

A. Antonelli, G. Bencivenni, G. Bologna [13], F. Bossi, P. Campana, G. Capon,
F. Cerutti, V. Chiarella, P. Laurelli, G. Mannocchi [14], F. Murtas,
G.P. Murtas, L. Passalacqua, M. Pepe-Altarelli [15]

Laboratori Nazionali dell'INFN (LNF-INFN), I-00044 Frascati, Italy

M. Chalmers, L. Curtis, J.G. Lynch, P. Negus, V. O'Shea, B. Raeven, C. Raine,
D. Smith, P. Teixeira-Dias, A.S. Thompson, J.J. Ward

Department of Physics and Astronomy, University of Glasgow, Glasgow G12 8QQ, UK [16]

O. Buchmüller, S. Dhamotharan, C. Geweniger, P. Hanke, G. Hansper, V. Hepp,
E.E. Kluge, A. Putzer, J. Sommer, K. Tittel, S. Werner [5], M. Wunsch

Institut für Hochenergiephysik, Universität Heidelberg, D-69120 Heidelberg, Germany [17]

R. Beuselinck, D.M. Binnie, W. Cameron, P.J. Dornan [15], M. Girone, S. Goodsir,
N. Marinelli, E.B. Martin, J. Nash, J. Nowell, J.K. Sedgbeer, P. Spagnolo,
E. Thomson, M.D. Williams

Department of Physics, Imperial College, London SW7 2BZ, UK [16]

V.M. Ghete, P. Girtler, E. Kneringer, D. Kuhn, G. Rudolph

Institut für Experimentalphysik, Universität Innsbruck, A-6020 Innsbruck, Austria [18]

A.P. Betteridge, C.K. Bowdery, P.G. Buck, P. Colrain, G. Crawford, G. Ellis,
A.J. Finch, F. Foster, G. Hughes, R.W.L. Jones, N.A. Robertson, M.I. Williams

Department of Physics, University of Lancaster, Lancaster LA1 4YB, UK [16]

P. van Gemmeren, I. Giehl, F. Hölldorfer, C. Hoffmann, K. Jakobs, K. Kleinknecht,
M. Kröcker, H.-A. Nürnberger, G. Quast, B. Renk, E. Rohne, H.-G. Sander,
S. Schmeling, H. Wachsmuth, C. Zeitnitz, T. Ziegler

Institut für Physik, Universität Mainz, D-55099 Mainz, Germany [17]

J.J. Aubert, C. Benchouk, A. Bonissent, J. Carr [15], P. Coyle, A. Ealet, D. Fouchez,
F. Motsch, P. Payre, M. Talby, M. Thulasidas, A. Tilquin

Centre de Physique des Particules, Faculté des Sciences de Luminy, IN2P3-CNRS, F-13288 Marseille, France

M. Aleppo, M. Antonelli, F. Ragusa

Dipartimento di Fisica, Università di Milano e INFN Sezione di Milano, I-20133 Milano, Italy

R. Berlich, V. Büscher, H. Dietl, G. Ganis, K. Hüttmann, G. Lütjens, C. Mannert,
W. Männer, H.-G. Moser, S. Schael, R. Settles, H. Seyerd, H. Stenzel,
W. Wiedenmann, G. Wolf

Max-Planck-Institut für Physik, Werner-Heisenberg-Institut, D-80805 München, Germany [17]

P. Azzurri, J. Boucrot, O. Callot, S. Chen, M. Davier, L. Duflot, J.-F. Grivaz,
Ph. Heusse, A. Jacholkowska, M. Kado, J. Lefrançois, L. Serin, J.-J. Veillet,
I. Videau [15], J.-B. de Vivie de Régie, D. Zerwas

Laboratoire de l'Accélérateur Linéaire, Université de Paris-Sud, IN2P3-CNRS, F-91898 Orsay Cedex, France

G. Bagliesi, S. Bettarini, T. Boccali, C. Bozzi, G. Calderini, R. Dell'Orso, I. Ferrante,
A. Giassi, A. Gregorio, F. Ligabue, A. Lusiani, P.S. Marrocchesi, A. Messineo,
F. Palla, G. Rizzo, G. Sanguinetti, A. Sciabà, G. Sguazzoni, R. Tenchini, C. Vannini,
A. Venturi, P.G. Verdini

Dipartimento di Fisica dell'Università, INFN Sezione di Pisa, e Scuola Normale Superiore, I-56010 Pisa, Italy

G.A. Blair, J. Coles, G. Cowan, M.G. Green, D.E. Hutchcroft, L.T. Jones, T. Medcalf,
J.A. Strong, J.H. von Wimmersperg-Toeller

Department of Physics, Royal Holloway & Bedford New College, University of London, Surrey TW20 OEX, UK [16]

D.R. Botterill, R.W. Clifft, T.R. Edgecock, P.R. Norton, J.C. Thompson

Particle Physics Dept., Rutherford Appleton Laboratory, Chilton, Didcot, Oxon OX11 OQX, UK [16]

B. Bloch-Devaux, P. Colas, B. Fabbro, G. Faïf, E. Lançon, M.-C. Lemaire, E. Locci, P. Perez, H. Przysieczniak, J. Rander, J.-F. Renardy, A. Rosowsky, A. Trabelsi [19], B. Tuchming, B. Vallage

CEA, DAPNIA / Service de Physique des Particules, CE-Saclay, F-91191 Gif-sur-Yvette Cedex, France [20]

S.N. Black, J.H. Dann, H.Y. Kim, N. Konstantinidis, A.M. Litke, M.A. McNeil, G. Taylor

Institute for Particle Physics, University of California at Santa Cruz, Santa Cruz, CA 95064, USA [21]

C.N. Booth, S. Cartwright, F. Combley, P.N. Hodgson, M.S. Kelly, M. Lehto, L.F. Thompson

Department of Physics, University of Sheffield, Sheffield S3 7RH, UK [16]

K. Affholderbach, A. Böhrer, S. Brandt, C. Grupen, A. Misiejuk, G. Prange, U. Sieler

Fachbereich Physik, Universität Siegen, D-57068 Siegen, Germany [17]

G. Giannini, B. Gobbo

Dipartimento di Fisica, Università di Trieste e INFN Sezione di Trieste, I-34127 Trieste, Italy

J. Putz, J. Rothberg, S. Wasserbaech, R.W. Williams

Experimental Elementary Particle Physics, University of Washington, Seattle, WA 98195, USA

S.R. Armstrong, E. Charles, P. Elmer, D.P.S. Ferguson, Y. Gao, S. González, T.C. Greening, O.J. Hayes, H. Hu, S. Jin, P.A. McNamara III, J.M. Nachtman [22], J. Nielsen, W. Orejudos, Y.B. Pan, Y. Saadi, I.J. Scott, J. Walsh, Sau Lan Wu, X. Wu, G. Zobernig

Department of Physics, University of Wisconsin, Madison, WI 53706, USA [23]

Abstract

Data collected at centre-of-mass energies of 181–184 GeV by ALEPH at LEP, corresponding to an integrated luminosity of 56.9 pb^{-1}, are analysed in a search for pair-produced charged Higgs bosons H$^{\pm}$. Three analyses are employed to select the $\tau^+ \nu_\tau \tau^- \bar{\nu}_\tau$, $c\bar{s}\tau^- \bar{\nu}_\tau/\bar{c}s\tau^+ \nu_\tau$ and $c\bar{s}s\bar{c}$ final states. No evidence for a signal is found. Mass limits are set as a function of the branching fraction B(H$^+ \to \tau^+ \nu_\tau$). Under the assumption that the decay modes considered cover the totality of the possible final states, charged Higgs bosons with masses below 59 GeV/c^2 are excluded at 95% C.L. independently of B(H$^+ \to \tau^+ \nu_\tau$). © 1999 Elsevier Science B.V. All rights reserved.

1. Introduction

Despite the success of the Standard Model of electroweak interactions in describing experimental observations, not much information is available about its cornerstone, the Higgs sector. In its minimal version, the Higgs mechanism is implemented by adding only one doublet of complex scalar fields, resulting in one additional physical scalar state, electrically neutral, commonly referred to as the standard Higgs boson. The most important phenomenological consequence of an extended Higgs structure is the appearance of additional physical spin-0 states [1]. For example, with the addition of one more doublet of complex scalar fields, five physical states remain

after spontaneous breaking of the $SU(2)_L \times U(1)_Y$ symmetry to give mass to $W^\pm$ and Z gauge bosons: three neutral and a pair of charged bosons. Among the possible choices, multi-doublet models are theoretically interesting because they automatically lead, at tree level, to $m_W = m_Z \cos\theta_W$ and to the absence of flavour changing neutral currents, two major constraints which must be satisfied by any extension of the Standard Model to agree with the experimental observations.

This letter describes a search for pair production in e^+e^- collisions of the charged Higgs bosons $H^\pm$ predicted in two-Higgs-doublet extensions of the Standard Model. The analysis uses the total integrated luminosity of 56.9 pb^{-1} collected in 1997 with the ALEPH detector at LEP, at centre-of-mass energies from 181 to 184 GeV, hereafter called the 183 GeV data.

Pair production of charged Higgs bosons occurs mainly via s-channel exchange of a photon or a Z boson; in two-doublet models, the couplings are completely specified in terms of the electric charge and θ_W, making the production cross section depend only on one additional parameter, the charged Higgs boson mass $m_{H^\pm}$. As expected in most implementations of multi-doublet models [1], it is assumed that H^+ decays, with negligible lifetime, predominantly into $c\bar{s}$ or $\tau^+\nu_\tau$ (and the respective charge conjugates for H^-). Additional decay channels, such as those involving neutral Higgs bosons, are not considered here. Since the relative weight of the two main channels depends on the details of the model, no assumption is made about the decay branching fractions, and three different selections are developed to address the possible final states $c\bar{s}s\bar{c}$, $c\bar{s}\tau^-\bar{\nu}_\tau/\bar{c}s\tau^+\nu_\tau$ (hereafter referred to as $c\bar{s}\tau^-\bar{\nu}_\tau$) and $\tau^+\nu_\tau\tau^-\bar{\nu}_\tau$. Under the same hypothesis, the negative results of the searches performed using 27.5 pb^{-1} collected at centre-of-mass energies ranging from 130 to 172 GeV allowed ALEPH to exclude charged Higgs boson masses less than 52 GeV/c^2 at 95% C.L., independently of the final state [2]. Using the data recorded at the same centre-of-mass energies, an excluded domain up to 54.5 GeV/c^2 has also been reported by DELPHI [3]. Charged Higgs boson masses up to 57.5 GeV/c^2 and 59.5 GeV/c^2 have been excluded by L3 [4] and OPAL [5], respectively, using their data recorded at centre-of-mass energies

up to 183 GeV. Less general limits have also been set by ALEPH [6], CLEO [7] and CDF [8].

The letter is organized as follows. After the description of the relevant parts of the ALEPH detector in Section 2, the event selections are detailed in Section 3. The results and the conclusions are given in Sections 4 and 5.

2. The ALEPH detector

The ALEPH detector is described in detail in Ref. [9]. An account of the performance of the detector and a description of the standard analysis algorithms can be found in Ref. [10]. Here, only a brief description of the detector components and of the algorithms relevant for this analysis is given.

In ALEPH, the trajectories of charged particles are measured with a silicon vertex detector, a cylindrical drift chamber, and a large time projection chamber. These are immersed in a 1.5 T axial field provided by a superconducting solenoidal coil. The electromagnetic calorimeter, placed between the tracking system and the coil, is a highly segmented sampling calorimeter which is used to identify electrons and photons and to measure their energies. The luminosity monitors extend the calorimetric coverage down to 34 mrad from the beam axis. The hadron calorimeter consists of the iron return yoke of the magnet instrumented with streamer tubes. It provides a measurement of hadronic energy and, together with the external muon chambers, muon identification.

The calorimetry and tracking information are combined in an energy flow algorithm, classifying a set of energy flow ''particles'' as photons, neutral hadrons and charged particles. Hereafter, charged particle tracks reconstructed with at least four hits in the TPC, and originating from within a cylinder of length 20 cm and radius 2 cm coaxial with the beam and centred at the nominal collision point, are referred to as *good tracks*.

3. Event selections

In order to ensure a good discovery potential independent of the branching fraction $B(H^+ \to \tau^+ \nu_\tau)$,

three selection procedures are designed for the topologies $\tau^+ \nu_\tau \tau^- \bar{\nu}_\tau$, $c\bar{s}\tau^- \bar{\nu}_\tau$ and $c\bar{s}s\bar{c}$. As in Ref. [2], the most relevant selection criteria for the three selections are chosen in order to achieve, on average and in case no signal is present, the best 95% C.L. limit on the $H^+ H^-$ production cross section. To do so, each selection is optimized individually with the most optimistic $B(H^+ \to \tau^+ \nu_\tau)$ in each case (100%, 50% and 0% for the $\tau^+ \nu_\tau \tau^- \bar{\nu}_\tau$, $c\bar{s}\tau^- \bar{\nu}_\tau$ and $c\bar{s}s\bar{c}$ channels, respectively, for which the combined contribution of the other two analyses is minimal),
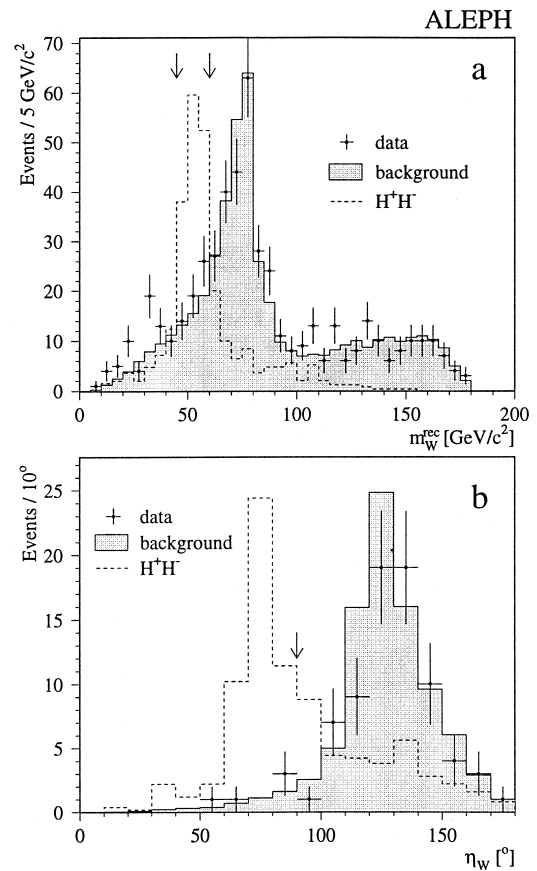
Fig. 1. Distribution of (a) the invariant mass of the quark jets and (b) their acollinearity angle used in the $c\bar{s}\tau^- \bar{\nu}_\tau$ global selection. The dots are the 183 GeV data, while the shaded histogram is the background expectation, normalized to the recorded luminosity. The dashed line is the distribution for a signal with a Higgs boson mass of 55 GeV/c^2, arbitrarily normalized. The arrows indicate the position of the cuts applied for this specific choice of the charged Higgs boson mass hypothesis (see text for details). Only a subset of the cuts is applied here to preserve sufficient statistics.

Table 1

Efficiencies ϵ (in%), numbers of Standard Model background events expected ($N_{\text{bkg}}^{\text{exp}}$) and subtracted ($N_{\text{bkg}}^{\text{sub}}$), and numbers of observed candidates (N_{obs}) for the three analyses at the centre-of-mass energy of 183 GeV, as functions of the charged Higgs boson masses (in GeV/c^2). For the mixed and four–jet channels, numbers are quoted within the windows defined by the sliding cuts, therefore implying some overlap among different charged Higgs boson mass hypotheses

$m_{\text{H}^\pm}$	Final state											
	$\tau^+\nu_\tau\tau^-\bar{\nu}_\tau$				$c\bar{s}\tau^-\bar{\nu}_\tau$				$c\bar{s}s\bar{c}$			
	ϵ	$N_{\text{bkg}}^{\text{exp}}$	$N_{\text{bkg}}^{\text{sub}}$	N_{obs}	ϵ	$N_{\text{bkg}}^{\text{exp}}$	$N_{\text{bkg}}^{\text{sub}}$	N_{obs}	ϵ	$N_{\text{bkg}}^{\text{exp}}$	$N_{\text{bkg}}^{\text{sub}}$	N_{obs}
50	40	6.5	5.0	4	37	1.2	1.0	2	37	5.6	5.0	5
55	42	6.5	5.0	4	34	1.3	1.0	1	36	6.8	6.1	4
60	43	6.5	5.0	4	31	1.5	1.2	2	35	7.9	7.0	11
65	45	6.5	5.0	4	25	2.1	1.7	3	33	8.8	7.9	9
70	46	6.5	5.0	4	20	3.1	2.5	6	32	10.5	9.4	14
75	48	6.5	5.0	4	18	5.1	4.1	5	31	19.1	17.0	20

following the prescription of Ref. [11] modified to include the possibility of partial or full background subtraction. In the following sections, the Monte Carlo samples used in designing the selections are described and the changes with respect to the analyses published in Ref. [2] are presented. In each case, the *subtractible* background, i.e., that for which the theoretical knowledge and the simulation accuracy are considered to be under control, is estimated together with the related systematic uncertainty.

3.1. Monte Carlo samples

Fully simulated Monte Carlo event samples reconstructed with the same program as the data have been used for background estimates, design of selections and cut optimization. Samples of all background sources corresponding to at least 20 times the collected luminosity were generated. The most important background sources are $e^+e^- \to \tau^+\tau^-$, $q\bar{q}$ and four-fermion processes (including W^+W^- production), simulated with KORALZ [12], PYTHIA [13] and KORALW [14].

The signal Monte Carlo events were generated using the HZHA [15] generator, extended for charged Higgs boson production as described in Ref. [2]. Samples of at least 1000 signal events were simulated for each of the various final states for charged Higgs boson masses between 40 and 80 GeV/c^2.

3.2. The $\tau^+\nu_\tau\tau^-\bar{\nu}_\tau$ final state

The final state produced by leptonic decays of both charged Higgs bosons consists of two acoplanar τ's and missing energy carried away by the neutrinos. Since this topology is very similar to that of stau pair production, the selection described in Ref. [16] is used here to search for charged Higgs bosons in the $\tau^+\nu_\tau\tau^-\bar{\nu}_\tau$ channel. This selection exploits the fact that the signal events contain at least four neutrinos, leading to large missing energy and a large acoplanarity of the visible system. Background from W^+W^- production followed by leptonic W decays is suppressed by vetoing events with energetic electrons or muons, which are softer when originating from τ decays.

Efficiencies to select events from $H^+H^- \to \tau^+\nu_\tau\tau^-\bar{\nu}_\tau$ are of the order of 45%, as shown in Table 1 for a representative set of Higgs boson masses. The

Table 2

Summary of the cuts applied in the $c\bar{s}\tau^-\bar{\nu}_\tau$ analyses. Units for masses and momenta are GeV/c^2 and GeV/c, respectively. Variables not defined in the text have the same meaning as in Ref. [2]

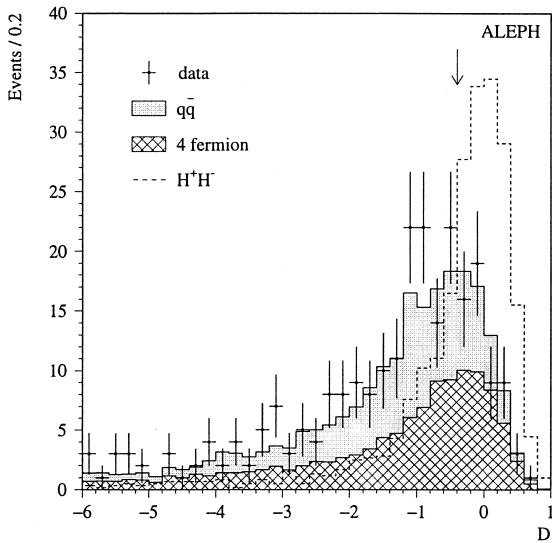| Preselection	
Good tracks	≥ 7
Visible mass m_{vis}	$[40, \sqrt{s}]$
Energy below 12°	$< 2.5\%\sqrt{s}$
Boost	> 0.3
$N_{\text{jet}}^{y=0.001}$	≥ 3
Global analysis	
Acoplanarity	$< 175°$
Thrust	< 0.9
E_{wedge}	$< 7.5\%\sqrt{s}$
P_{T}	$> 20\% E_{\text{vis}}$
$P_{\text{e},\mu}$	< 24
$m_{\text{vis}}^{\text{NO e},\mu}$	< 80
Tau identification	loose
η_{W}	$< [35 + m_{\text{H}^\pm}]°$
$m_{\text{W}}^{\text{rec}}$	$[m_{\text{H}^\pm} - 10, m_{\text{H}^\pm} + 5]$
Topological analysis	
θ_{miss}	$[25.8°, 154.2°]$
E_{wedge}	$< 20\%\sqrt{s}$
$P_{\text{e},\mu}$	< 24
$m_{\text{vis}}^{\text{NO e},\mu}$	< 80
Tau identification	tight
η_{H}	$< [40 + m_{\text{H}^\pm}]°$
$m_{\text{H}}^{\text{rec}}$	$[m_{\text{H}^\pm} - 15, m_{\text{H}^\pm} + 5]$

Fig. 2. The distribution of the discriminant variable D used in the $c\bar{s}s\bar{c}$ selection. Shown are data (points with error bars), Monte Carlo for the expected background sources (cumulative histograms, normalized to the recorded luminosity) and the Monte Carlo expectation for a signal with $m_{H^{\pm}} = 55$ GeV/c^2 (dashed histogram, arbitrary normalization). The arrow indicates the position of the cut applied. Some cuts have been relaxed to preserve sufficient statistics.

total background expected amounts to 6.5 events, consisting mainly of irreducible background from $W^+W^- \to \tau^+\nu_\tau\tau^-\bar{\nu}_\tau$. In the data, four events were selected, in good agreement with the Standard Model expectation. For the interpretation of the negative result of the search in terms of mass limits, the part of the expected background coming from W^+W^- is

Table 3
Summary of the cuts applied in the $c\bar{s}s\bar{c}$ analysis. Units for masses and momenta are GeV/c^2 and GeV/c, respectively. The preselection variables have been defined in Ref. [2]

Four-jet preselection	
Good Tracks	> 7
Charged Energy	$> 10\% \sqrt{s}$
$P_{z-\text{axis}}$	$< 1.5[m_{\text{vis}} - 90]$
$E_{\text{jet}}^{\text{em}}$	$< 90\% E_{\text{jet}}$
Y_{34}	> 0.003
Thrust	< 0.9
Equal mass and spin-0 constraints	
$\theta_{\text{prod}}, \theta_{\text{dec},i}, \chi^2_{5C}, c_{\text{tag}}$	$D \geq -0.4$

subtracted; the latter amounts to 5.0 events, including a reduction of 3% to account for systematic uncertainties [16].

3.3. The $c\bar{s}\tau^-\bar{\nu}_\tau$ final state

The mixed final state, $c\bar{s}\tau^-\bar{\nu}_\tau$, is characterized by two jets originating from the hadronic decay of one of the charged Higgs bosons and a thin τ jet plus missing energy due to the neutrinos from the decay of the other.

Two complementary approaches are used to select the mixed final state: in one selection, called the *global* analysis, global quantities such as acoplanarity, thrust, and missing momentum are predominantly used whereas the second selection, referred to as the *topological* analysis, relies more on the specific τ jet reconstruction. As the analyses are described in detail in Ref. [2], the focus here is on changes other than a simple rescaling of the cuts with $\sqrt{s}$.

As $m_{H^{\pm}}$ approaches m_W the sensitivity of both analyses is limited by the W^+W^- background. Two changes are introduced to improve the rejection of
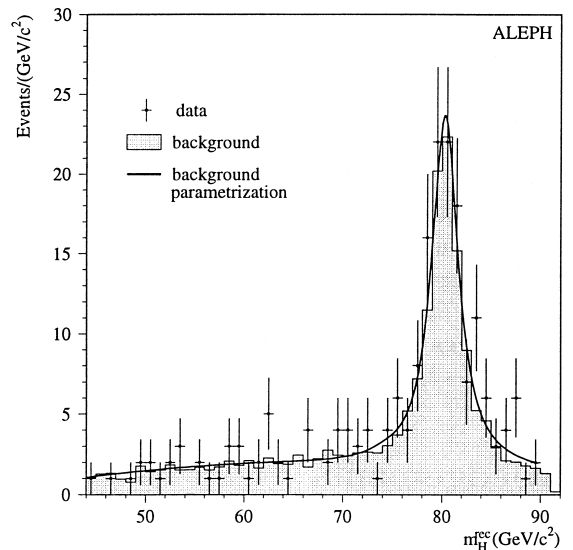

Fig. 3. Distribution of the dijet mass m_H^{rec} obtained after applying all cuts of the $c\bar{s}s\bar{c}$ selection; shown are 130–183 GeV data (dots with error bars), background Monte Carlo (shaded histogram) and the background parametrization used in deriving the limits (solid line).

this background. The first change concerns the momentum of the leading lepton (electron or muon) which is now required to be less than 24 GeV/c in both analyses.

The second change involves the rejection of the $\tau\nu q\bar{q}'$ final state of W pair events: cuts are introduced which depend on the signal mass hypothesis (*sliding* cuts) and are tightened with increasing $m_{H^\pm}$.

In the global analysis the rejection is achieved with cuts on the acollinearity angle η_W of the two hadronic jets and their invariant mass m_W^{rec}. The acollinearity angle is required to be less than $[35 + m_{H^\pm}/(\text{GeV}/c^2)]$ degrees. The event is rejected if the

invariant mass lies outside the range of $[m_{H^\pm} - 10\,\text{GeV}/c^2, m_{H^\pm} + 5\,\text{GeV}/c^2]$. The good agreement of data and Monte Carlo in these two variables is shown in Fig. 1.

In the topological analysis the invariant mass m_H^{rec} of the two jets assigned to the Higgs boson must lie in a window between $m_{H^\pm} - 15\,\text{GeV}/c^2$ and $m_{H^\pm} + 5\,\text{GeV}/c^2$. Their acollinearity η_H must be less than $[40 + m_{H^\pm}/(\text{GeV}/c^2)]$ degrees.

The complete set of cuts is listed in Table 2. As in Ref. [2], events are accepted if they pass either analysis. Typical efficiencies and background expectations are given in Table 1. The main contributions
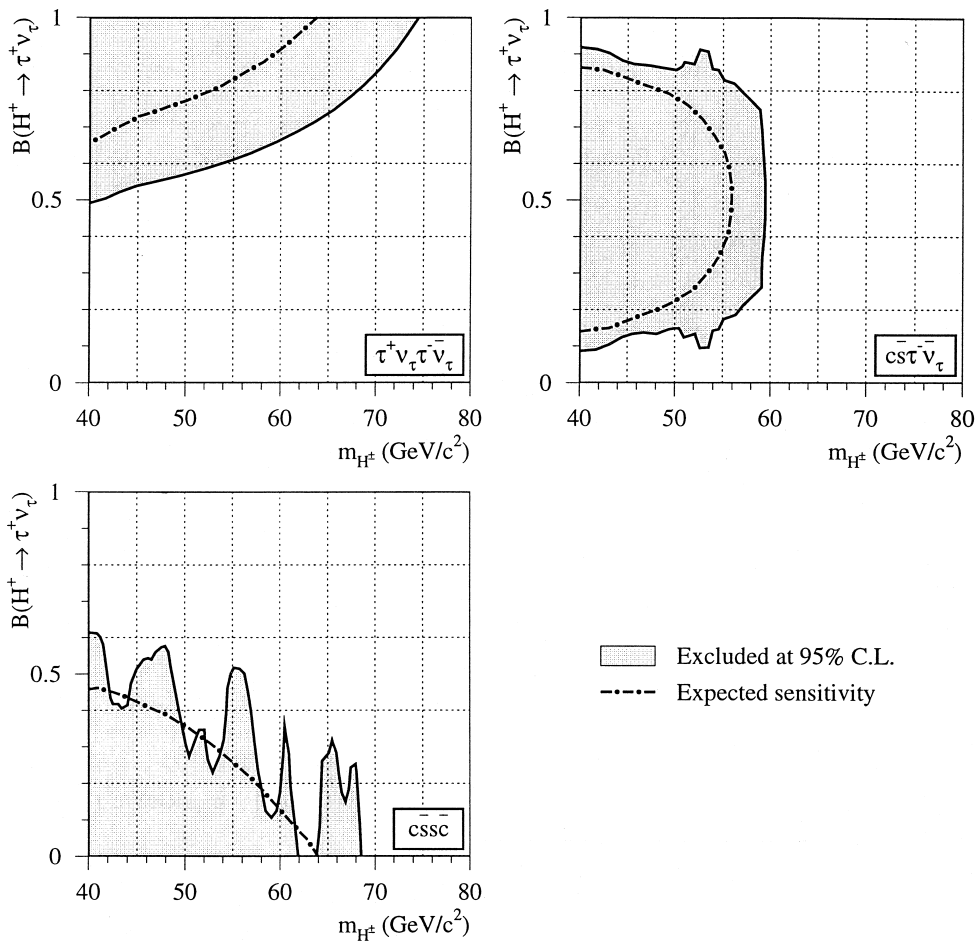

Fig. 4. Limit at 95% C.L. on the mass of charged Higgs bosons as a function of $B(H^+ \rightarrow \tau^+ \nu_\tau)$ from each of the three individual analyses. Shown are the expected (dash-dotted curves) and observed (shaded areas) 95% C.L. exclusion domains.

to the systematic error (3%) on the efficiency are: Monte Carlo statistics; the luminosity measurement accuracy (< 1%); the uncertainty (< 2%) on the knowledge of the inefficiency introduced by beam related energy deposits at polar angles below 12°, studied using events triggered at random beam crossings.

Nine events were selected in the data for Higgs boson masses from 40 to 75 GeV/c^2, in agreement with the background expectation of 8.7.

For the determination of the result, the W^+W^- background, representing 93% of the total contamination, is reduced by a systematic error of 13% and subtracted. Here the systematic error represents the statistical precision of a test of the W^+W^- Monte Carlo for masses reconstructed in the region of the expected sensitivity. The test is performed using a data sample dominated by the W^+W^- process, selected by relaxing the cuts on the hadronic acollinearity and on the energy of the leading lepton and requiring the hadronic mass to be less than 75 GeV/c^2. In the data, 63 events were observed, in agreement with the expectation of 73.5 events.

3.4. The $c\bar{s}s\bar{c}$ final state

For this channel, the hadronic decays of the two charged Higgs bosons lead to a final state with four well separated jets. With respect to Ref. [2], the preselection applied to identify four-jet final states and the choice of jet pairing are unchanged, but the variables discriminating signal and Standard Model processes are exploited in a different way to face the larger W^+W^- background. These variables are

· the production polar angle θ_{prod} between the Higgs boson momentum direction and the beam axis;
· the decay angles $\theta_{dec,i}$ ($i = 1,2$) in the rest frame of the two reconstructed $H^\pm$ candidates;
· the chi squared χ^2_{5C} of the 5C-fit.

In addition, a c-jet tagging variable c_{tag} is introduced to take advantage of the presence of c quarks in the signal decay products. This variable is the output of a neural network trained to discriminate c-jets from light quark jets. The lifetime and specific decay modes of D mesons as well as jet-shape properties are exploited. A detailed description can be found in Ref. [17].

The four variables are combined linearly into one discriminant observable:

$$D = -\cos^2\theta_{prod} + 0.4\,c_{tag} - 0.2\,\text{Min}(\cos\theta_{dec,i})^2 - 0.6\,\chi^2_{5C}.$$

The distribution of D is shown in Fig. 2. Events are accepted if $D \geq -0.4$.

The selection cuts are summarized in Table 3. After these cuts, the total background expected for reconstructed charged Higgs boson masses lower than 75 GeV/c^2 amounts to 42.8 events. Efficiencies are of the order of 35% within a dijet mass window of ± 3 GeV/c^2 around the Higgs boson mass hypothesis, as shown in Table 1.

As in Ref. [2], given the level of irreducible background, the sensitivity of the analysis is considerably increased by subtracting the expected background from Standard Model processes. For this purpose the dijet mass distribution as obtained from the background Monte Carlo is parametrized by the sum of a polynomial and a Breit-Wigner distributions. The comparison with the data (Fig. 3) shows
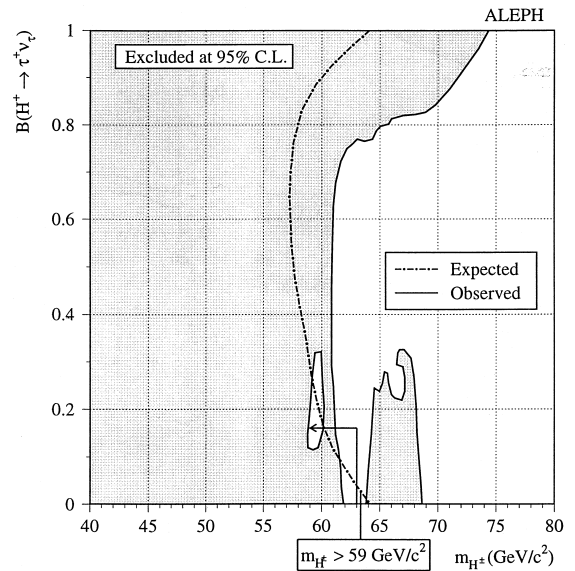

Fig. 5. Limit at 95% C.L. on the mass of charged Higgs bosons as a function of B($H^+ \to \tau^+\nu_\tau$) from the combination of the three individual analyses. Shown are the expected (dash-dotted curve) and observed (shaded area) 95% C.L. exclusion domains. The hole between 59 and 60 GeV/c^2 and with B($H^+ \to \tau^+\nu_\tau$) ~ 0.2 is actually excluded at 90% C.L.

that the parametrization is consistent with the observation. In the following, the subtracted background is conservatively reduced by 11%, corresponding to the statistical uncertainty of this comparison.

The systematic error on the number of signal events expected is estimated to be 2%, dominated by the Monte Carlo statistical uncertainty, with small additional contributions from the luminosity measurement and possible inaccuracies in the simulation of the energy flow reconstruction.

4. Results

The number of candidate events observed in the data collected at centre-of-mass energies from 181 to 184 GeV are given in Table 1 for different charged Higgs boson masses and for each of the three analyses presented in Section 3. A total of 60 events is retained for $m_{H^{\pm}} < 75$ GeV/c^2, consistent with the 57.9 events expected from Standard Model processes. Since, in addition, the mass distribution in the c$\bar{s}$s$\bar{c}$ channel does not show any significant accumulation outside the W region (Fig. 3), the results of the three selections described in this note are combined with those obtained using 130–172 GeV data to set an improved 95% C.L. lower limit on the charged Higgs boson mass, following the procedure described in Ref. [18] for the combination of the confidence levels and the prescription of [19] for the background subtraction.

The separate results of the three analyses are displayed in Fig. 4, where the contours corresponding to expected (dash-dotted curves) and observed (solid curves) confidence levels of 5% (equivalent to a 95% C.L. exclusion) are drawn. For B(H$^+ \rightarrow \tau^+ \nu_{\tau}$) = 0, 0.5 and 1, values maximizing in turn the weight of the three channels c$\bar{s}$s$\bar{c}$, c$\bar{s}\tau^- \bar{\nu}_{\tau}$ and $\tau^+ \nu_{\tau}\tau^- \bar{\nu}_{\tau}$, 95% C.L. lower limits on $m_{H^{\pm}}$ are set to 62, 59.5 and 74.5 GeV/c^2.

The result of the combination of the three analyses is displayed in Fig. 5. Charged Higgs bosons with masses less than 59 GeV/c^2 are excluded at 95% confidence level independently of B(H$^+ \rightarrow \tau^+ \nu_{\tau}$), in agreement with the expected exclusion sensitivity of 57 GeV/c^2.

5. Conclusions

The search for pair-produced charged Higgs bosons in the three final states $\tau^+ \nu_{\tau}\tau^- \bar{\nu}_{\tau}$, c$\bar{s}\tau^- \bar{\nu}_{\tau}$ and c$\bar{s}$s$\bar{c}$ has been updated using 56.9 pb^{-1} of data collected at $\sqrt{s} = 181 - 184$ GeV. No evidence of Higgs boson production was found and new mass limits were set as a function of B(H$^+ \rightarrow \tau^+ \nu_{\tau}$). When combined with data recorded at centre-of-mass energies from 130 to 172 GeV, charged Higgs bosons with masses below 59 GeV/c^2 are excluded at 95% C.L. independently of B(H$^+ \rightarrow \tau^+ \nu_{\tau}$).

References

[1] J.F. Gunion, H.E. Haber, G. Kane, S. Dawson, The Higgs Hunter's Guide, Frontiers in Physics, Lecture Note Series, Addison Wesley, 1990.

[2] ALEPH Collaboration, Phys. Lett. B 418 (1998) 419.

[3] DELPHI Collaboration, Phys. Lett. B 420 (1998) 140.

[4] L3 Collaboration, Search for Charged Higgs Bosons in $e^+ e^-$ Collisions at Centre-of-Mass Energies between 130 and 183 GeV, CERN-EP/98-149, 1998, submitted to Phys. Lett. B.

[5] OPAL Collaboration, Search for Higgs bosons in $e^+ e^-$ Collisions at 183 GeV, CERN-EP/98-173, 1998, submitted to Eur. Phys. J.C.

[6] ALEPH Collaboration, Phys. Lett. B 343 (1995) 444.

[7] CLEO Collaboration, Phys. Rev. Lett. 74 (1995) 2885.

[8] CDF Collaboration, Phys. Rev. Lett. 79 (1997) 357.

[9] ALEPH Collaboration, Nucl. Instrum. and Methods A 294 (1990) 121.

[10] ALEPH Collaboration, Nucl. Instrum. and Methods A 360 (1995) 481.

[11] J.-F. Grivaz, F. Le Diberder, Complementary Analyses and Acceptance Optimization in new Particle Searches, LAL preprint # 92-37, 1992.

[12] S. Jadach, B.F.L. Ward, Z. Wąs, Comp. Phys. Commun. 79 (1994) 503.

[13] T. Sjöstrand, The PYTHIA 5.7 and JETSET 7.4 Manual, LU-TP 95/20, CERN-TH 7112/93, Comp. Phys. Commun. 82 (1994) 74.

[14] M. Skrzypek, S. Jadach, W. Placzek, Z. Wąs, Comp. Phys. Commun. 94 (1996) 216.

[15] G. Ganis, P. Janot, The HZHA Generator in: G. Altarelli, T. Sjöstrand, F. Zwirner (Eds.), Physics at LEP2, CERN 96-01, 1996, vol. 2, p. 309.

[16] ALEPH Collaboration, Phys. Lett. B 433 (1998) 176.

[17] ALEPH Collaboration, Measurement of $|V_{cs}|$ in hadronic W decays, ALEPH 98-011, CONF 98-001, available from http://alephwww.cern.ch/ALPUB/.

[18] P. Janot, F. Le Diberder, Nucl. Instrum. and Methods A 411 (1998) 449.

[19] S. Jin, P. McNamara, The Signal Estimator Limit Setting Method, physics/9812030, submitted to Nucl. Instrum. and Methods A.